# Stationary bumps in networks of spiking neurons

Carlo R. Laing[1] and Carson C. Chow[2]
Department of Mathematics,
University of Pittsburgh, Pittsburgh PA 15260

October 10, 2000

**Abstract**

We examine the existence and stability of spatially localized "bumps" of neuronal activity in a network of spiking neurons. Bumps have been proposed in mechanisms of visual orientation tuning, the rat head direction system, and working memory. We show that a bump solution can exist in a spiking network provided the neurons fire asynchronously within the bump. We consider a parameter regime where the bump solution is bistable with an all-off state and can be initiated with a transient excitatory stimulus. We show that the activity profile matches that of a corresponding population rate model. The bump in a spiking network can lose stability through partial synchronization either to a traveling wave or to the all-off state. This can occur if the synaptic time scale is too fast through a dynamical effect or if a transient excitatory pulse is applied to the network. A bump can thus be activated and deactivated with excitatory inputs which may have physiological relevance.

## 1 Introduction

Neuronal activity due to recurrent excitations in the form of a spatially localized pulse or bump has been proposed as a mechanism for feature selectivity in models of the visual system (e.g. Somers *et al.*, 1995; Hansel and Sompolinsky, 1998), the head direction system (Skaggs *et al.*, 1995; Zhang, 1996; Redish *et al.*, 1996), and working memory (Wilson and Cowan, 1973; Amit and Brunel, 1997; Camperi & Wang, 1998). Much of the previous mathematical formulations of such structures have employed population rate models (Wilson & Cowan, 1972, 1973; Amari, 1977; Kishimoto & Amari, 1979; Hansel and Sompolinsky, 1998). See Ermentrout (1998) for a recent review.

Here, we consider a network of spiking neurons that shows such structures and investigate their properties. In our network we find localized time–stationary states (bumps) which may be analogous to the structures measured in the experiments of e.g. Colby *et al.* (1995) and

[1]Present Address: Dept of Physics, University of Ottawa, Ottawa, Ontario, Canada K1N 6N5.
[2]To whom correspondences should be addressed. Email: ccc@math.pitt.edu

Funahashi *et al.* (1989) . The network is bistable with the bump and the "all–off" state both being stable. Note that the neurons are not intrinsically bistable as in Camperi & Wang (1998) and the bump solutions do not arise from a Turing–Hopf instability like that studied by Bressloff & Coombes (1998) and Bressloff *et al.* (1999), i.e. there is no continuous path in parameter space connecting a bump and the all–off state. A time–stationary solution is one which corresponds to asynchronous firing of neurons where the firing rate is constant at each spatial point but the rate depends on spatial location. We show that the activity profile of the bumps of our model are the same as that of a corresponding population rate model.

However, bumps predicted by the rate model to be stable may in fact be unstable in a model which includes the spiking dynamics of the neurons. The rate model implicitly assumes asynchronous firing and only considers the dynamics of the firing rate. As the synaptic decay time is increased in the spiking network the bump can lose stability as a result of temporal correlation or "partial synchronization" of neurons involved in the bump. If the initial conditions are symmetric then this synchronization causes the input to the neurons to drop below the threshold required to keep it firing, leading to cessation of oscillation of the neurons and consequently the rest of the bump. However, for generic initial conditions or with the inclusion of noise, the bump destabilizes to a traveling wave. For fast enough synapses, the wave cannot exist. If some heterogeneity in the intrinsic properties of the neuron is included then the bump can be "pinned" to a fixed location; the traveling wave does not form and the bump loses stability to the all-off state.

This instability provides a mechanism for the termination of a bump, as would be required at the end of a memory task (e.g. the delayed saccade task discussed by Colby *et al.* (1995)): if many of the neurons involved in the bump can be caused to fire approximately simultaneously, and the synaptic time scale is short, there will not be enough input after this coincident firing to sustain activity and the network will switch to the all-off state.

# 2 Neuron model

We consider a network of $N$ integrate–and–fire neurons whose voltages, $v_i$, obey the differential equations

$$\frac{dv_i}{dt} = I_i - v_i + \sum_{j,m} \frac{J_{ij}}{N} \alpha(t - t_j^m) - \sum_l \delta(t - t_i^l), \tag{1}$$

where the subscript $i$ indexes the neurons, $t_j^m$ is the $m$th firing of neuron $j$, defined by the times that $v_j(t)$ crosses the threshold which we have set to 1, $I_i$ is the input current applied to neuron $i$, and $\delta(\cdot)$ is the Dirac delta function, which resets the voltage to zero. The function $\alpha(t)$ is a post-synaptic current and is nonzero only for $t > 0$. The connection weight between neuron $i$ and neuron $j$ is $J_{ij}$. The sum over $m$ and $l$ extend over the entire firing history of the neurons in the network and the sum over $j$ extends over the network. Each time the voltage crosses the threshold from below the neuron is said to "fire". The voltage then immediately resets to $v_i = 0$ and a synaptic pulse $\alpha(t)$ is sent to all connected neurons.

In our examination of bump solutions we will consider subthreshold input ($I_i < 1$) and a weight matrix that is translationally invariant (i.e. $J_{ij}$ only depends on $|i - j|$). It is of the lateral inhibition form (i.e. locally excitatory but distally inhibitory); this type of

connectivity matrix can be shown to arise from a multi–layer network with both inhibitory and excitatory populations if the inhibition is fast, as shown by Ermentrout (1998).

We can formally integrate Eq. (1) to obtain the spike response form (Gerstner, 1995; Gerstner *et al.*, 1996; Chow, 1998). This form will allow us to relate the bump profile for the integrate–and–fire network to the profile of a rate model similar to that studied by Amari (1977). Suppose that neuron $i$ has fired in the past at times $t_i^l$, where $l = 0, -1, -2, \ldots, -\infty$. The neuron most recently fired at $t_i^0$. We consider the dynamics for $t > t_i^0$. Integrating Eq. (1) yields

$$v_i(t) = I_i(1 - e^{-(t-t_i^0)}) + \sum_{j,m} \frac{J_{ij}}{N} \int_{t_i^0}^{t} e^{s-t} \alpha(s - t_j^m)\, ds, \tag{2}$$

By breaking up the integral in (2) into two pieces we obtain

$$v_i(t) = I_i(1-e^{-(t-t_i^0)}) + \sum_{j,m} \frac{J_{ij}}{N} \int_{-\infty}^{t} e^{s-t} \alpha(s-t_j^m)\, ds - e^{-(t-t_i^0)} \sum_{j,m} \frac{J_{ij}}{N} \int_{-\infty}^{t_i^0} e^{s-t_i^0} \alpha(s-t_j^m)\, ds, \tag{3}$$

from which we obtain the spike response form

$$v_i(t,s) = I_i - [I_i + u_i(s)]e^{-(t-s)} + u_i(t), \qquad t > s, \qquad v_i(s,s) = 0 \tag{4}$$

where

$$u_i(t) = \sum_{j,m} \frac{J_{ij}}{N} \epsilon(t - t_j^m), \tag{5}$$

and

$$\epsilon(t) = \int_0^t e^{s-t} \alpha(s) ds. \tag{6}$$

We normalize $\epsilon(t)$ so that $\int_0^\infty \epsilon(t)\, dt = 1$. Note that for low rates of firing $[I + u_i(s)]e^{-(t-s)} \simeq e^{-(t-s)}$.

## 2.1 Numerical Methods

We performed numerical simulations of the integrate–and–fire network using the spike response form Eq. (2). We step Eq. (2) forward using a fixed time step, $\Delta t$, until one or more of the voltages is above threshold (set to be 1). Assume e.g. that $v_i([n+1]\Delta t) > 1$ while $v_i(n\Delta t) < 1$, for some $n$. At this point, a backwards linear interpolation in voltage is made to determine the approximate firing time of neuron $i$. To determine the approximate correct value of $v_i([n+1]\Delta t)$, we then make an Euler step from the approximate last firing time of neuron $i$ to time $[n+1]\Delta t$, using (1) for the slope. The equations are then stepped forward again.

The domain is the unit interval with periodic boundary conditions, and the weight function involves a difference of Gaussians — see Fig. 1 for an example. For the synaptic pulse, $\alpha(t)$, we take

$$\alpha(t) = \beta \exp(-\beta t) \tag{7}$$

so that

$$\epsilon(t) = \frac{\beta[e^{-t} - e^{-\beta t}]}{\beta - 1} \tag{8}$$

The parameter $\beta$ affects the rate at which the post–synaptic current decays. Noise is added to the network as current pulses to each neuron of the form

$$I_{\text{rand}}(t) = 6(e^{-10t} - e^{-15t})$$

where $t \geq 0$. The arrival times of these pulses have a Poisson distribution with mean frequency 0.05 and there is no correlation between pulse arrival times for different neurons.

# 3 Existence of the bump state

We examine the existence of bump solutions to the spike response system described by (4). A bump solution is spatially localized with spatially dependent average firing rate of the participating neurons. The firing rate is zero outside the bump and rises from zero at the edges to a maximum in the center. The firing times of the neurons are uncorrelated, so the bump is a localized patch of incoherent or asynchronous firing. The state coexists with the homogeneous non–firing (all–off) state.

It is convenient to define the activity of neuron $i$ as

$$A_i(t) = \sum_l \delta(t - t_i^l), \tag{9}$$

where the sum over $l$ is over all past firing times. Our activity differs from the population activity of Gerstner (1995) which considers the activity of an infinite pool of neurons at a given spatial location. We can then rewrite the synaptic input (5) in terms of the activity as

$$u_i(t) = \sum_j \frac{J_{ij}}{N} \int_0^\infty \epsilon(s) A_j(t-s)\ ds \tag{10}$$

Consider stationary asynchronous solutions to the spike response equations. Many authors have studied the spatially homogeneous asynchronous state with various coupling schemes (Abbott and van Vreeswijk, 1993; Treves, 1993; Gerstner, 1995, 1998, 2000). Our approach is similar to that of Gerstner (1995, 1998, 2000). We first rewrite the activity as

$$A_i(t) = A_i^0 + \Delta A_i(t), \tag{11}$$

where

$$A_i^0 = \lim_{\tau\to\infty} \frac{1}{\tau} \int_0^\tau A_i(r) dr. \tag{12}$$

Substituting (9) into (12) then yields $A_i^0 = \lim_{\tau\to\infty} n(\tau)/\tau$, where $n(\tau)$ is the number of times neuron $i$ fired in the time interval $\tau$. Thus, $A_i^0$ is the mean firing rate of neuron $i$.

We now insert (11) into (10) to obtain $u_i(t) = u_i^0 + \Delta u_i(t)$ where

$$u_i^0 = \sum_j \frac{J_{ij}}{N} A_j^0, \tag{13}$$

and

$$\Delta u_i(t) = \sum_j \frac{J_{ij}}{N} \int_0^\infty \epsilon(s) \Delta A_j(t-s) ds \tag{14}$$

(recall that $\int_0^\infty \epsilon(s)\, ds = 1$). We define the asynchronous state to be one where $\Delta u_i(t)$ is zero in the limit of infinite network size $N$. In the asynchronous state the input to neuron $i$ is a constant and given by $u_i^0$. This implies that the firing times of the neurons are uncorrelated. For a finite system, $\Delta u(t)$ will contribute fluctuations which scale as $N^{-1/2}$.

We now derive the self-consistent equations for the asynchronous state. Substitute $u_i(t) = u_i^0$ into (4); the local firing period $(A_i^0)^{-1}$ will be given by

$$v_i((A_i^0)^{-1} + s, s) = 1 = I_i - [I_i + u_i^0]e^{-(A_i^0)^{-1}} + u_i^0. \tag{15}$$

Solving (15) yields

$$A_i^0 = G[u_i^0] \tag{16}$$

where

$$G[z] = \begin{cases} 0, & z \le 1 - I \\ -1/\ln\left[\frac{I+z-1}{I+z}\right], & z > 1 - I \end{cases} \tag{17}$$

(A plot of $G[z]$ can be seen in Fig. 2.) This form is similar to the usual neural network rate equation, (e.g. Amari, 1977; Kishimoto & Amari, 1979; Hansel & Sompolinsky, 1998; Ermentrout, 1998) except that the gain function we have derived is a result of the intrinsic neuronal dynamics of our model (Gerstner, 1995). Combining (13) and (16) we obtain the condition for a stationary asynchronous solution

$$u_i^0 = \sum_j \frac{J_{ij}}{N} G[u_j^0], \tag{18}$$

For a finite sized system, the time averaged firing rate of the neurons follows a profile given by $A_j^0 = G[u_j^0]$.

We first consider mean-field solutions to (18). We assume that $u_i^0 = u^0$, $I_i = I$ and $\sum J_{ij}/N = J$ yielding

$$u^0 = JG[u^0] \tag{19}$$

If $I > 1$ (oscillatory neurons), then there are no solutions if $J$ is too large and one solution if $J$ is small enough. For $I < 1$ (excitatory neurons), (19) has one solution at $u_0 = 0$ if $J$ is too small and two solutions if $J$ is large enough (See Fig. 2, which shows the case $J = 2$). These two states correspond to an 'all-off' state and an 'all-on' state respectively.

## 3.1 Bump State

In order for a bump to exist, a solution to (18) for $u_i^0$ must be found such that $u_i^0 + I_i$ is above threshold ($u_i^0 + I_i > 1$) in a localized region of space. We show example figures of such solutions in Figs. 3 and 4. Amari (1977) and Kishimoto & Amari (1979) proved that such a solution can exist for a class of gain functions $G[z]$. Similar to the mean field solution, we find that for subthreshold input ($I_i < 1$), the all-off state always exists and the bump state can exist if the weight function has enough excitation. We will discuss stability of the bump in Sec. 4. Stability will be affected by the synaptic time scale, the weight function, the amount of applied current and the size of the network. For a finite sized system, we show in Appendix A that the individual neurons in a bump do not fire with a fixed spatially dependent period. These finite sized fluctuations act as a source of noise.

As noted by Gerstner (1995, 1998), the spike response model can be connected to classical neural network or population rate models (Wilson and Cowan, 1972; Amari, 1977; Hopfield, 1984). If we choose $\epsilon(s) = e^{-s}$, which is true for $\alpha(t) = \delta(t)$, and assume near synchronous firing so that $A_i(t) \simeq G[u_i(t)]$, then by differentiating (10) with respect to time we obtain:

$$\frac{d}{dt}u_i(t) = -u_i(t) + \sum_j J_{ij}G[u_j(t)] \tag{20}$$

This is the classical neural network or population rate model. Amit and Tsodyks (1991), Gerstner (1995) and Shriki *et al.* (1999) have previously shown that networks of spiking neurons can be represented with rate models provided there does not exist a large degree of synchrony. The condition for a stationary solution for (20) is identical to (18). If the synapse has a more complicated time course such as a difference of exponentials then a higher order rate equation could be derived (Ermentrout, 1998). The activity is a functional of the input as well as a function of time. The assumption made in deriving (20) is that the explicit time dependence of the activity is weak compared to the dependence on the input $u_i(t)$. This is valid only for weakly synchronous or correlated firing. For strongly synchronous firing, the explicit time dependence of the activity would dominate the functional dependence on the inputs.

### 3.2 Numerical simulations

We compare stationary bump profiles obtained from both (20) and a network of integrate–and–fire neurons. A space-time raster plot of the firing times of a stationary bump from a simulation of a network of 100 integrate–and–fire neurons is shown in Fig. 3. The network was switched into the bump state by applying a transient spatially localized current for sufficient time to excite the bump. This state has a large basin of attraction — as long as neurons are excited in a localized region, the network relaxes into a bump of the form shown in Fig. 3. The raster plot shows that the bump is localized in space and persists for many firing times. The neurons in the center of the bump fire much faster than those near the edges.

Fig. 4 shows the profile of the average firing rate (activity) for the integrate–and–fire system (2) with three different values of $\beta$ and no noise. The solid line corresponds to the theoretically predicted profile from (18). This corresponds to the stable stationary solution of the corresponding rate model (20), with the gain function (17). The comparison for $\beta$ small (i.e. slow synapses) is excellent, while as $\beta$ is increased the agreement lessens but is still very good. We also have found bumps in a networks of conductance-based neurons (results not shown, see Gutkin *et al.* (2000) for an example). We find that the existence of a bump solution for a network of spiking neurons to be robust.

## 4 Stability and the synaptic time scale

In order for the bump to be observable it must be stable to perturbations. A stability analysis of the spike response system can be performed by considering the linear behavior of small perturbations around the stationary bump state. However, for the spatially inhomogeneous

bump, this computation is quite involved. Instead, we infer the conditions for stability of the bump from a stability analysis of the homogeneous asynchronous state of the spike response model and confirm our conjectures with numerical simulations.

Stability of the bump state has previously been examined in a first order rate model. Amari (1977) and Kishimoto & Amari (1979) found for saturating gain functions, that the stability of the bump in the rate model depended on a relationship between the weight function and the applied current. Hansel & Sompolinsky (1998) find the stability constraints for a model with a simplified weight function on a periodic domain and a piecewise linear gain function. However, as discussed in Sec. 3.1 the rate model is only valid for infinitely fast synapses and asynchronously firing neurons. If correlations develop between firing times of neurons, the rate model is no longer valid.

It has been shown previously for homogeneous networks (Abbott & Van Vreeswijk, 1993; Treves, 1993; Gerstner, 1995, 1998, 2000) that the asynchronous state of a network of integrate-and-fire neurons is unstable to oscillations with fast excitatory coupling. Gerstner (1998, 2000) has shown that oscillations will develop at harmonics of the average firing rate (activity). The addition of noise helps to stabilize the asynchronous state. However, for low to moderate levels of noise, a fast enough synapse can still cause an instability. These calculations are based on perturbing the stationary asynchronous state for an infinite number of neurons using a Fokker-Planck or related integral formalism. We note that there are two sources of noise in the simulations. The first is the randomly arriving currents, $I_{\rm rand}$, and the second is the fluctuations due to the finite size of the network. The latter is a manifestation of unpredictability in a high dimensional deterministic dynamical system.

The integrate–and–fire network has a parameter, $\beta$, which controls the time scale of the synaptic input. We find that varying $\beta$ has a profound effect on the stability of the bump solution. If $\beta$ is slowly increased (i.e. the synaptic time–scale is slowly shortened) while all other parameters are held constant, the bump will eventually lose stability. The initial location of a bump is determined by the spatial structure of the initial current stimulation. If the initial condition is symmetric and no noise is added the bump will remain in place and then lose stability directly to the all-off state at a critical value of $\beta$. However, as a result of the invariance of the network under spatial translations, a bump is marginally stable with respect to spatial translation, i.e. there is a continuum of attractors parameterized by their spatial location, rather than a finite set of isolated attractors. A consequence of this marginal stability is that a bump may "wander" under the influence of noise and/or finite size fluctuations. With asymmetric initial conditions and/or noise, the bump will begin to wander as $\beta$ is increased (see Fig. 5). (Fig. 10 shows the bump wandering for a fixed value of $\beta$.)

At a larger value of $\beta$ the wandering bump loses stability to a traveling wave. Note that the wave speed increases as $\beta$ increases. The same type of behavior was observed for larger networks (results not shown). If the wave hits an obstruction then it will switch to the all-off state. The bump can be pinned in place if a small amount of disorder or heterogeneity is included in the input current. In Fig. 6 we have added disorder by randomly choosing the fixed currents, $I_i$, keeping the average of these values across the network equal to the value used in Fig. 5. The bump migrates to a local maximum in the current and remains there. For sufficiently large $\beta$, it destabilizes into the all-off state as in Fig. 6. The pinning due to disorder is sufficiently strong that traveling waves cannot persist. Note that small patches

of neurons can be activated by noise, but they cannot persist if $\beta$ is too large.

We conjecture that the loss of stability in the bump for large $\beta$ is due to a loss of stability of the asynchronous bump state due to the synchronizing tendency of the neurons with fast excitatory coupling as is seen in the homogeneous network. Integrate-and-fire neurons belong to what is known as Type I or Class I neurons (Hansel *et al.*, 1995; Ermentrout, 1996). It is known that for Type I neurons, fast excitation has a synchronizing tendency whereas slow excitation has a desynchronizing tendency (Van Vreeswijk *et al.*, 1994; Gerstner, 1995; Hansel *et al.*, 1995). Chow (1998) showed that a network with heterogeneous input is still able to synchronize.

The stationary bump corresponds to an asynchronous network state where the neurons receive heterogeneous input. For fast enough excitatory coupling, the asynchronous state might lose stability and oscillations will develop. The synchronous oscillations need not be exceptionally strong. All that is required is that large enough oscillations develop and induce a traveling wave. For symmetric initial conditions, the symmetry prevents the formation of a traveling wave. The neurons oscillate in place and for enough synchronization, the synaptic input is not at a high enough level to push some of the neurons in the bump above threshold when it is time for them to fire. The bump solution would then collapse and switch the network to the all-off state. This also occurs for the case with heterogeneity. The pinned bump develops stationary oscillations and switches to the all-off state.

For a fixed weight function, we find that when $I$ is at a value for which the rate model predicts the bump to be stable, the bump in the integrate–and–fire network is stable for small $\beta$, but becomes unstable as $\beta$ increases. This is shown in Fig. 7, where we show the region of the $I-\beta$ plane in which there is a stable bump solution in the integrate–and–fire network with no noise for $N = 100$. The stability region, as well as size and shape of the bump, depends on the applied current $I$, the weight function $J(x)$, and the size of the network, but is unchanged by adding noise of the intensity used in other simulations in this paper.

The finite size fluctuations are important for the dynamics. Fig. 8 shows a plot of $u_i(t)$ at the center of a bump containing 100 neurons for two different values of $\beta$. The traces show noisy oscillations at a given frequency around an average value. The dominant frequency of the oscillations is at the neuron's average firing rate. As $\beta$ increases, the amplitude of the noisy oscillations increase. We conjecture that the increase in the size of the oscillations is partially due to the dynamical synchronizing effect described above. For small $N$, the noisy oscillations are dominated by finite size fluctuations but for large $N$ it will be dominated by the synchronizing effect of the fast excitation. We believe that the destabilizing effect of the oscillations will be present even for infinite $N$. While increasing $N$ does decrease the the size of the fluctuations, this is more than compensated by the the increase in oscillation size due to increasing $\beta$. In Fig. 9 we plot the maximum value of $\beta$ for which a bump is stable as a function of $N$ for various noise values. The plot shows that the stability boundary asymptotes for a fixed value of $\beta$ for large values of $N$. This plot suggests that for any $N$, there is a finite $\beta$ above which the bump is no longer stable even in the presence of noise. As expected the bump can tolerate higher levels of $\beta$ as the noise level increases although the maximum $\beta$ seems to saturate as noise increases.

From Figs. 4 and 8 we see that as $\beta$ is increased, the activity and mean value of $u$ at each neuron decreases slightly despite the fact that we have compensated the synaptic strength so the integrated synaptic input is constant. We believe that this small decrease is a result

of the fluctuations in the input due to the finite number of neurons and the synchronizing dynamical effect. The termination of the bump as $\beta$ is increased is not due to this overall decrease in synaptic input. If the coupling weight is increased to keep the mean value of $u$ constant (by multiplying $J(z)$ by a factor slightly greater than 1), the bump is still seen to terminate as $\beta$ is increased. Indeed, numerical results suggest that the mean value of $u$ decreases linearly (albeit weakly) with $\beta$ while its standard deviation increases at a faster than linear rate (results not shown).

# 5 Initiating and terminating bumps

Since bumps are thought to be involved in such areas as working memory [Colby *et al.* (1995), Funahashi *et al.* (1989)] and head direction systems [Redish *et al.* (1996), Zhang (1996)], understanding their dynamics on a time scale much longer than the period of oscillation of the individual neurons is important. In particular, being able to "turn on" and "turn off" a bump is of interest. Since the input current $I$ is subthreshold, the network is bistable, the two stable states being the bump and the all–off state where none of the neurons fire. Turning the bump on is simply a matter of shifting the system from the all-off state into the basin of attraction of the bump. This is done by applying a spatially–localized input current to the already–existing uniform current for a short period of time — on the order of 5 oscillation periods of the neuron in the center of the bump (whose activity is highest), as shown in Fig. 10. Note that the bump persists after the stimulation has been removed.

As we have seen, partially synchronizing the neurons can cause the bump to terminate. One mechanism for causing some of the neurons to synchronize is to apply a brief, strong excitatory current to most or all of the neurons involved in the bump. This will cause a number of the neurons to fire together, i.e. be temporarily synchronized, leading to termination of the bump if the synapse is fast enough. An example of this is shown in Fig. 10, where a short stimulus is applied to all of the neurons involved in the bump, although not to all of the neurons in the network. The stimuli to turn on and turn off the bump are both excitatory, i.e. the stimulus to turn off a bump does not have to be inhibitory, although that is also successful.

The reason the bump turns off is a dynamical effect. An alternate means of turning off the bump with excitation is to utilize the lateral inhibition in the network. If the parameters are tuned correctly then a strong excitatory input to all of the neurons in the network will induce enough inhibition to reduce the synaptic input below threshold and extinguish the bump. As discussed in Sec. 4, the bump is seen to wander in Fig. 10. A small amount of disorder could prevent this occurrence by pinning the bump to a given location. We explore the initiation and termination of bumps more carefully in a companion publication (Gutkin *et al.*, 2000).

# 6 Discussion and Conclusions

We have shown that a one–dimensional network of spiking neurons can sustain spatially–localized bumps of activity and that the profiles of the bumps agree with those predicted

by a corresponding population rate model. However, when the synapses occur on a fast time scale, bumps can no longer be sustained in the network. They either lose stability to traveling waves or completely switch off. We also find that heterogeneity or disorder can pin the bumps to a single location and keep them from wandering. We conjecture that the loss of stability of the bump is due to partial synchronization between the neurons. It is known for homogeneous networks of Type 1 neurons that fast excitatory synapses have a synchronizing tendency. We use this instability to turn off bumps with a brief excitatory stimulus to partially synchronize the neurons.

For the network sizes that we have probed, we have found that bumps can be sustained by synapses with decay rates as fast as three to four times the firing rate of the fastest neurons in the bump. If we consider neurons in the cortex to be firing at approximately 40 Hz this would correspond to synaptic decay times of the order of 5 to 10 ms which is not unreasonable. Results with conductance-based neurons have found that the synaptic time scale can be sped up to well within the AMPA range and still sustain a bump state (Gutkin *et al.*, 2000). We also find that as the network size increases, the bump may tolerate faster synapses. While the stability of the bump depends crucially on the synaptic time scale, the activity profile of the bump depends only on the connection weights and the gain function. Thus, it may be possible to make predictions on the connectivity patterns of experimental cortical systems from the firing rates of the neurons within the bump and the firing rate (F-I) curve of individual neurons.

If these recurrent bumps are involved in working memory tasks then our results lead to some experimental predictions. For example if it is possible to pharmacologically speed up the excitatory excitations in the cortex, bump formation and hence working memory may be perturbed. A brief applied stimulus applied to the cortical area where the working memory is thought to be held may also disrupt a working memory task.

Among other authors who have produced similar work are Hansel & Sompolinsky (1998), Bressloff *et al.* (1999) and Compte *et al.* (1999). Hansel & Sompolinsky (1998) consider a rate model similar to that studied by Amari (1977) and Kishimoto & Amari (1979), using a piece–wise linear gain function (our $G[z]$) and retaining only the first two Fourier components of the weight function $J$, which allows them to make analytic predictions about the transitions between different types of behavior. They also show the existence of a bump in a network of conductance–based model neurons and show that bumps can following moving spatially–localized current stimulations, a feature that may be relevant for head–direction systems such as those studied by Redish *at al.* (1996) and Zhang (1996).

Bressloff & Coombes (1998) and Bressloff *et al.* (1999) study pattern formation in a network of coupled integrate–and–fire neurons, but their systems consider suprathreshold input ($I_i > 1$) so that the all–off state is not a solution. They find that by increasing the coupling weight between neurons the spatially–uniform synchronized state (all neurons behave identically) becomes unstable through a Turing–Hopf bifurcation, leading to spatial patterns similar to those shown in Fig. 4. They find bistability between a bump and a spatially–uniform synchronized state, whereas we find bistability between a bump and the all–off state. This difference is crucial if the system is to be thought of as modeling working memory as investigated by, among others, Colby *et al.* (1995) and Funahashi *et al.* (1989).

Compte *et al.* (1999), have demonstrated the existence of a bump attractor in a two-layer network of excitatory and inhibitory integrate–and–fire neurons. Their network involves

strong excitation and inhibition in a balanced state. It is possible that a corresponding rate model could be found for this network to obtain the shape of the profile. They were also able to switch the bump off and on with an excitatory stimulus. However, it is believed that their switching off mechanism is due to the inhibitory input induced from the excitation provided.

We have also observed bumps in two–dimensional networks. A number of other authors, e.g. Fohlmeister *et al.* (1995) and Horn & Opher (1997), have investigated two–dimensional networks of integrate–and–fire neurons, but not in the context of bumps. Preliminary investigations (results not shown) indicate that bumps can be initiated and terminated in two–dimensional networks in exactly the same fashion as for one–dimensional networks. We emphasize that while the bumps are spatially localized they need not be contiguous. It may be such that a certain amount of disorder in the synaptic connectivity would lead to a bump that is distributed over a given region. This disorder may even confer some beneficial effects by breaking the translational symmetry and keep the bump from wandering when under the influence of stochastic firing. We hope to elucidate these effects in the future.

# 7 Acknowledgments

We wish to thank D. Pinto and G.B. Ermentrout for stimulating discussions that spurred this research. We also thank A. Compte and N. Brunel for some clarifying conversations. We especially thank Boris Gutkin for many fruitful discussions and for his critical insight. This work was supported in part by the National Institutes of Health (CC), and the A.P. Sloan Foundation (CC).

# A Non periodicity of bump solutions

Here we show that locally periodic solutions are not possible for a bump in a finite sized integrate-and-fire network. We consider the ansatz of periodic firing given by $t_i^{m_i} = (\phi_i - m_i)T_i$, where $\phi_i$ is a phase, $m_i$ is an integer, and $T_i$ is the local firing period. We suppose that the neuron previously fired at $t_i^{-1}$ and will next fire at $t_i^0$. We now substitute this ansatz into the firing equation (4) to obtain

$$1 = I_i - [I_i - u_i(t_i^{-1})]e^{-T_i} + u_i(t_i^0), \tag{21}$$

where

$$u_i(t) = \int J_{ij} \sum_{m_j} \epsilon(t - (\phi_j - m_j)T_j) \tag{22}$$

In order to find a solution for $T_i$ that is constant in time, we require $u_i(t)$ to be constant or $T_i$ periodic in $t$. However, $\sum_{m_j} \epsilon(t-(\phi_j - m_j)T_j) \equiv f(t)$ is $T_j$ periodic and $T_j$ is not constant in $j$ for a bump solution. This implies that $u_i(t)$ cannot be $T_i$ periodic for all $i$ (except for infinite $N$ or for highly singular cases where all the periods are rationally related). Hence, a locally periodic bump solution is not possible for the finite sized spike response model and hence for the integrate–and–fire network.

# References


[1] Abbott L.F. and Van Vreeswijk, C. 1993. Asynchronous states in a network of pulse-coupled oscillators. *Phys. Rev. E* **48**, 1483-1490.

[2] Amari, S. 1977. Dynamics of pattern formation in lateral–inhibition type neural fields. *Biol. Cybern.* **27**, 77-87.

[3] Amit, D.J. and Tsodyks, M.V. 1991. Quantitative study of attractor neural network retrieving at low spike rates: I. Substrate – spikes, rates and neuronal gain. *Network* **2**, 259-273.

[4] Amit, D.J. and Brunel, N. 1997. Model of global spontaneous activity and local structured activity during delay periods in the cerebral cortex. *Cereb. Cortex* **7** 237-252.

[5] Bressloff, P. C. and Coombes, S. 1998. Spike train dynamics underlying pattern formation in integrate–and–fire oscillator networks. *Phys. Rev. Lett.* **81** (11), 2384-2387.

[6] Bressloff, P. C., Bressloff, N. W., and Cowan, J. D. 1999. Dynamical mechanism for sharp orientation tuning in an integrate–and–fire model of a cortical hypercolumn. Preprint 99/13, Department of Mathematical Sciences, Loughborough University.

[7] Camperi M. and Wang X.-J. 1998 A model of visuospatial working memory in prefrontal cortex: recurrent network and cellular bistability. *J. Comput. Neurosci.* **5** 383-405.

[8] Chow, C.C. 1998. Phase–locking in weakly heterogeneous neuronal networks. *Physica D* **118**, 343-370.

[9] Colby, C. L., Duhamel, J.-R., and Goldberg, M. E. 1995. Oculocentric Spatial Representation in Parietal Cortex. *Cerebral Cortex.* **5**, 470-481.

[10] Compte, A., Brunel, N., Wang, X.-J. 1999. Spontaneous and spatially tuned persistent activity in a cortical working memory model. 1999. Abstract, Computational Neuroscience Meeting 1999.

[11] Ermentrout, G.B. 1996. Type I membranes, phase resetting curves, and synchrony. *Neural Comp.* **8**, 979-1001.

[12] Ermentrout, G.B. 1998. Neural networks as spatio–temporal pattern–forming systems. *Reports on progress in physics.* **61**(4), 353-430.

[13] Fohlmeister, C., Gerstner, W., Ritz, R., and van Hemmen, J. L. 1995. Spontaneous Excitations in the Visual Cortex: Stripes, Spirals, Rings and Collective Bursts. *Neural Comp.* **7**(5), 905-914.

[14] Funahashi, S., Bruce, C. J. and Goldman–Rakic, P. S. 1989. Mnemonic coding of visual space in the monkey's dorsolateral prefrontal cortex. *J. Neurophysiology.* **61**(2), 331-349.

[15] Gerstner, W. 1995. Time structure of the activity in neural network models . *Phys. Rev.* E, **51** 738-758.

[16] Gerstner, W., van Hemmen, J.L., and Cowan, J. 1996. What matters in neuronal locking? *Neural Comput.* **8**, 1653-1676.

[17] Gerstner, W. 1998. Populations of spiking neurons. n: W. Maass and C.M. Bishop (Editors), Pulsed Neural Networks, MIT press, pp. 261-295.

[18] Gerstner, W. 2000. Population Dynamics of Spiking Neurons: Fast Transients, Asynchronous States, and Locking. *Neural Comput.* **12** 43-89.

[19] Gutkin B.S., Laing C.R., Chow, C.C., Colby, C., and Ermentrout, G.B. 2000. Turning on and off with excitation: the role of spike-timing asynchrony and synchrony in sustained neural activity. Preprint.

[20] Hansel, D., Mato, G., and Meunier,C. 1995. Synchrony in excitatory neural networks. *Neural Comp.* **7**, 307-335.

[21] Hansel, D. and Sompolinsky, H. 1998. Modeling feature selectivity in local cortical circuits, in *Methods in Neuronal Modeling.* Second edition, ed. C. Koch and I. Segev. MIT Press, 1998.

[22] Hopfield, J.J. 1984. Neurons with graded response have collective computational properties like those of two-state neurons. *Proc. Natl. Acad. Sci. USA* **81**, 3088-3092.

[23] Horn, D. and Opher, I. 1997. Solitary Waves of Integrate–and–Fire Neural Fields. *Neural Comp.* **9**(8), 1677-1690.

[24] Kishimoto, K. and Amari, S. 1979. Existence and stability of local excitations in homogeneous neural fields. *J. Math. Biology* **7**, 303-318.

[25] Kistler, W.M., Seitz, R., and van Hemmen, J.L. 1998. Modelling Collective Excitations in Cortical Tissue. Physica D, **114**, 273-295.

[26] Redish, A. D., Elga, A. N. and Touretzky, D. S. 1996. A coupled attractor model of the rodent head direction system. *Network* **7**(4), 671-685.

[27] Shriki, O., Sompolinsky, H., and Hansel, D. 1999. Rate models for conductance based cortical neuronal networks. Preprint.

[28] Skaggs, W. E., Knierim, J. J., Kudrimoti, H. S. and McNaughton, B. L. 1995. A model of the neural basis of the rat's sense of direction. In G. Tesauro, D. Touretzky, T. Leen, (Eds.), Advances in neural information processing systems, Vol. 7 (pp. 173-180). MIT Press.

[29] Somers D.C., Nelson, S.B., and Sur, M. An emergent model of orientation selectivity in cat visual cortical simple cells. *J. Neuroscience* **15**, 5448 – 5465.

[30] Traub, R., Wong, R., Miles, R. and Michelson, H. 1991. A model of a CA3 hippocampal pyramidal neuron incorporating voltage–clamp data on intrinsic conductances. *J. Neurophysiol.* **66**, 635-649.

[31] Treves, A. 1993. Mean-field analysis of neuronal spike dynamics. *Network* **4**, 259-284.

[32] Van Vreeswijk, C., Abbott, L.F., and Ermentrout, G.B. 1994. *J. Comp. Neurosci.* **1**, 313-321.

[33] Wilson H.R. and Cowan J.D. 1972. Excitatory and inhibitory interactions in localized populations of model neurons. *Biophysical J.* **12**, 1-24.

[34] Wilson H.R. and Cowan J.D. 1973. A mathematical theory of the functional dynamics of cortical and thalamic nervous tissue *Kybernetic* **13**, 55-80.

[35] Zhang, K. 1996. Representation of spatial orientation by the intrinsic dynamics of the head–direction cell ensembles: A theory. *J. Neuroscience* **16**, 2112-2126.

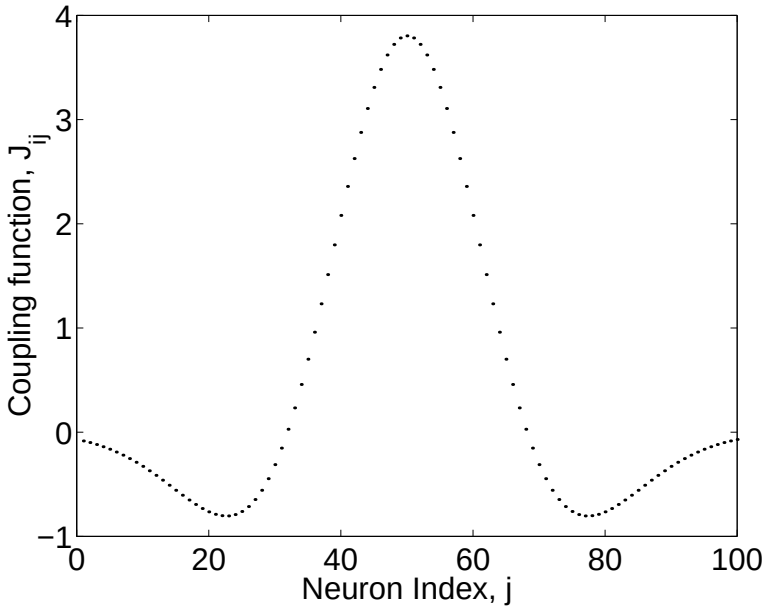


Figure 1: The weight function $J_{ij} = NJ(|i-j|/N)$ for $i = 50$ and $N = 100$, where $J(z) = 5[1.1w(1/28, z) - w(1/20, z)]$, and $w(a, z) = (a\pi)^{-1/2} \exp(-z^2/a)$.

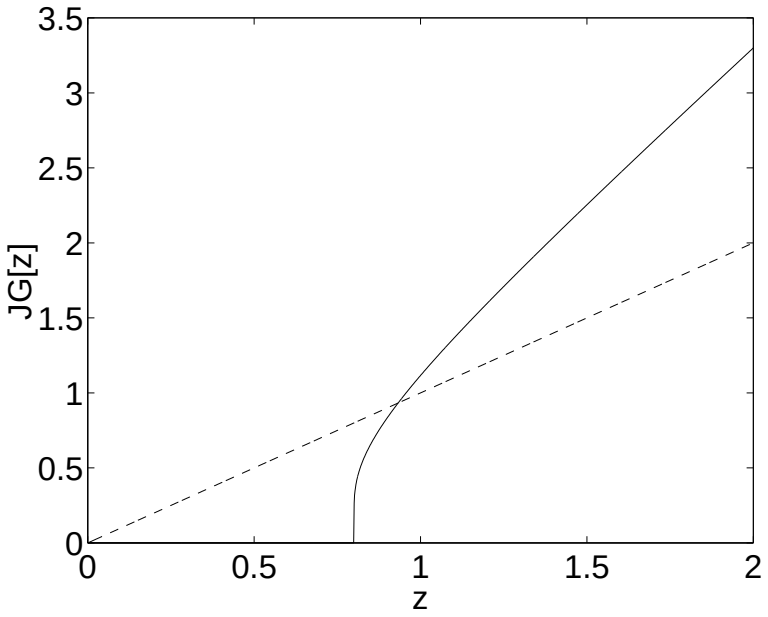


Figure 2: A multiple ($J$) of the gain function $G[z]$ (Eq. (17)) (solid line) for $I = 0.2$ and $J = 2$, and the diagonal (dashed). The threshold occurs at $z = 1 - I$, when 1 is the voltage threshold for the integrate–and–fire neuron. The intersection of the dashed line and the gain function gives the mean-field solution to Eq. (19).

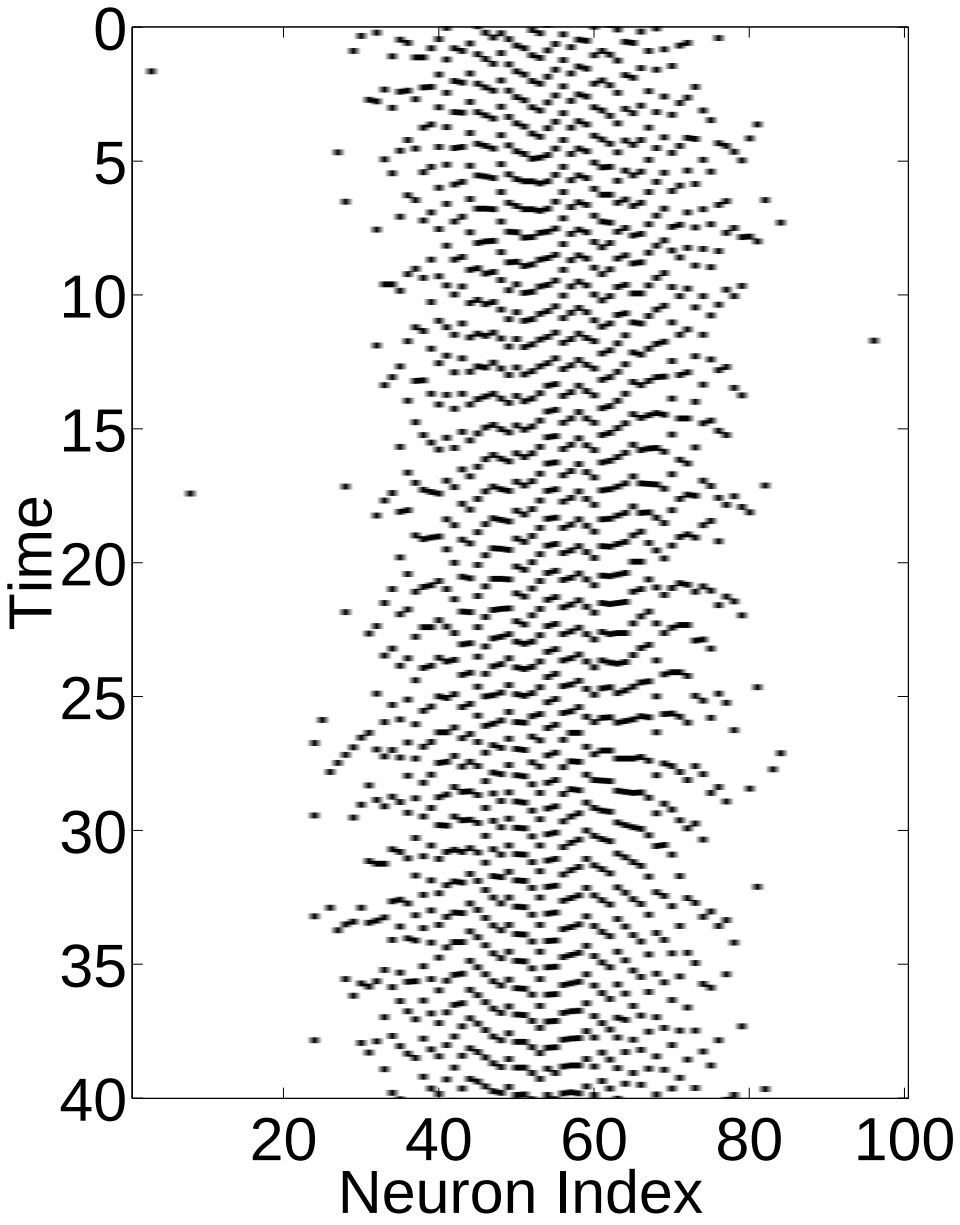


Figure 3: An example of a stationary bump. The dots represent the firing times of a network of 100 neurons. Noise in the form of random current pulses with a mean frequency of 0.05 as discussed in Sec. 2.1 was included in the simulation . Parameter values used were: $\beta = 1.5$, $I = 0.9$, and $J_{ij}$ as in Fig. 1.

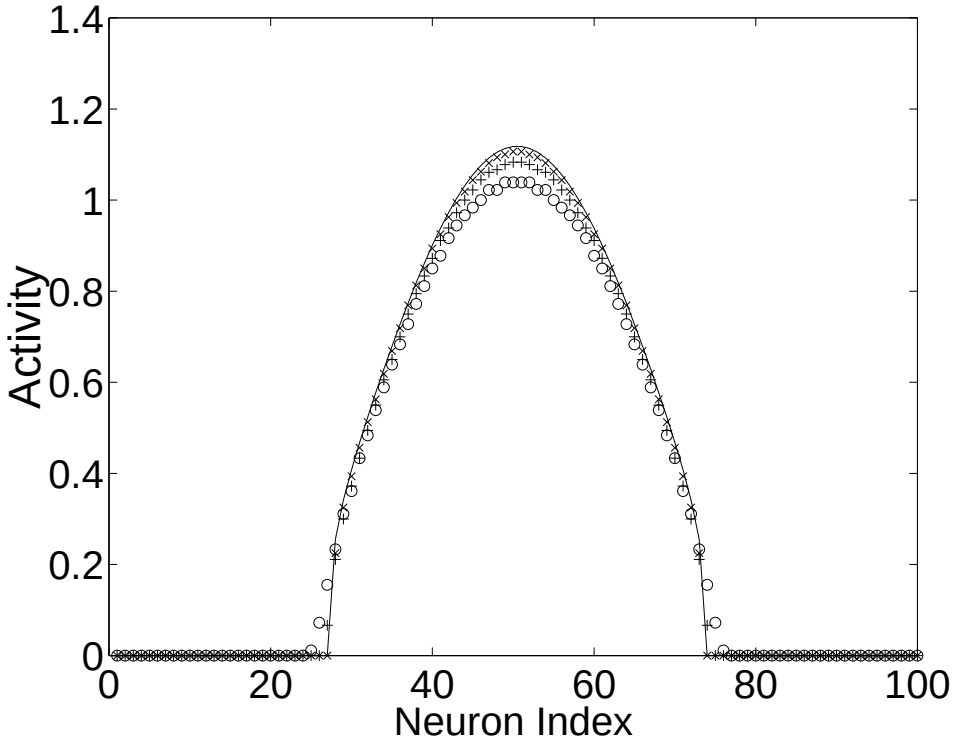


Figure 4: The activity profile (mean firing rate) for $\beta = 2.5$ ($\circ$), $\beta = 1.5$ ($+$) and $\beta = 0.5$ ($\times$) for the integrate–and–fire network, and for the rate model Eq. (20) (solid line). $I = 0.9$ and the weight function is as in Fig. 1. Note that for smaller $\beta$ the agreement between the firing rate model and the integrate–and–fire model is better. The errors in the activity values are all less than 0.01.

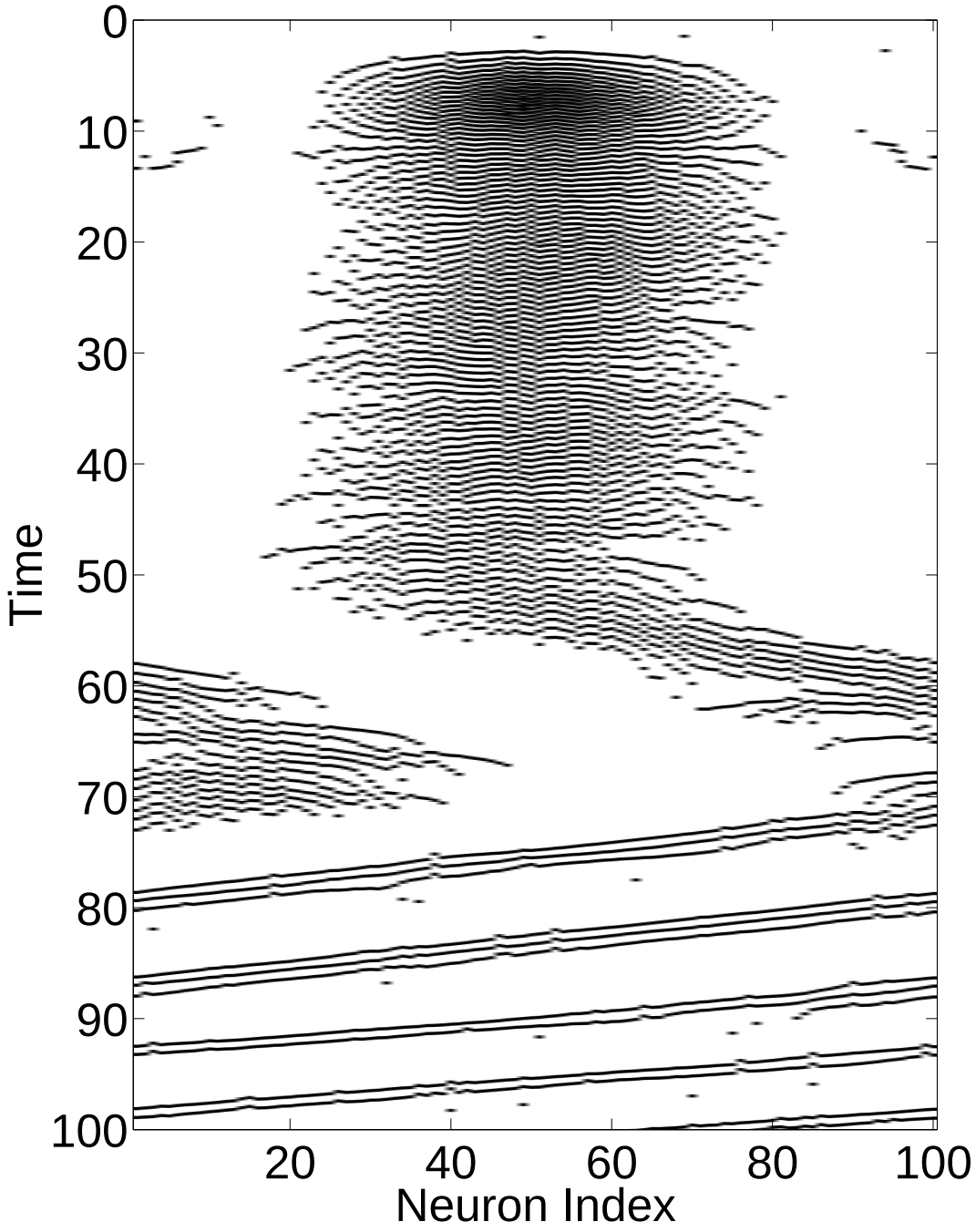


Figure 5: Bump destabilization due to quasistatic increase of $\beta$. Here, $\beta$ is linearly increased in time from $\beta = 3.1$ at the top of the figure to $\beta = 8.3$ at the end. The weight function is $J(z) = 5[1.16w(1/28, z) - w(1/20, z)]$ (see caption of Fig. 1 for the definition of $w$), $I = 0.8$, and the noise is as in Fig. 3. Bump loses stability first to wandering then to a traveling wave.

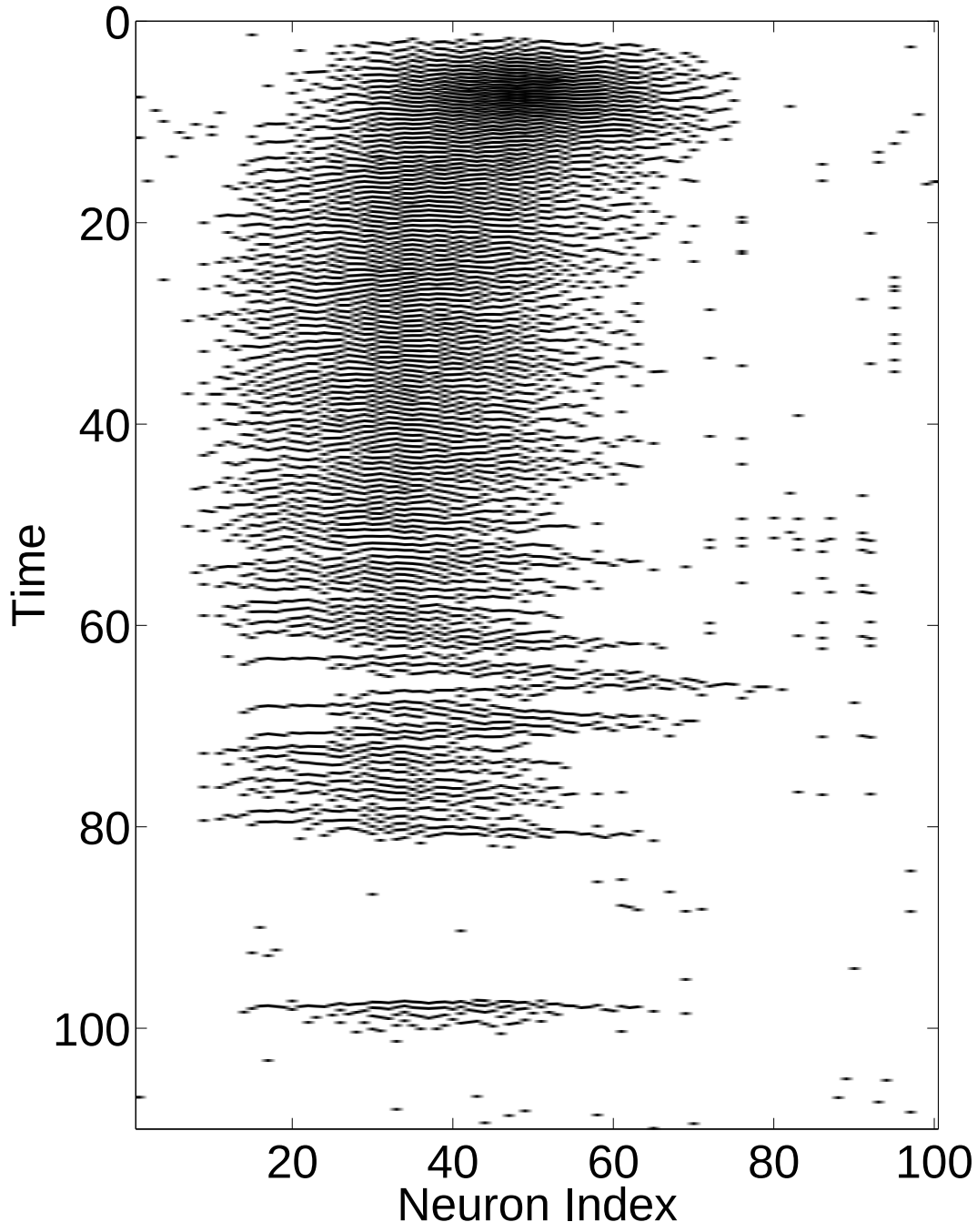


Figure 6: Bump destabilization due to quasistatic increase of $\beta$ with disorder added to the static background current. The range of $\beta$, the weight function, the noise, and the average value of $I$ are as in Fig. 5. Disorder pins the bump and prevents the formation of a traveling wave.

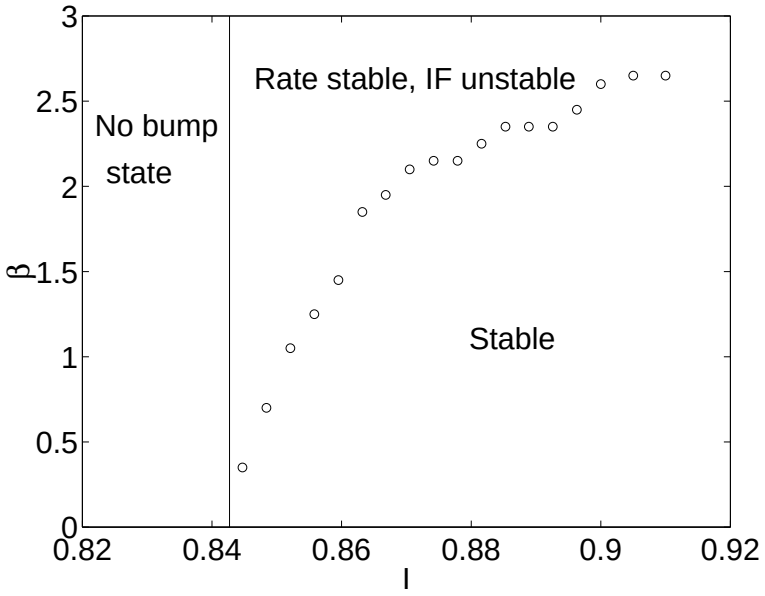


Figure 7: Numerically obtained stability boundary (circles) for a bump in the noise–free integrate-and-fire model for $J_{ij}$ as in Fig. 1 and $N = 100$, as a function of $I$ and $\beta$. The bump is stable below the curve marked by circles. The solid line shows the existence region for the bump in the rate model: it exists to the right but not to the left of the line. Above the curve marked by circles the bump exists and is stable in the rate model but unstable in the integrate and fire model. As discussed in the text, the curve marked by circles will move to larger $\beta$ as $N$ is increased. This curve is not significantly changed when noise of the level used in the other simulations shown is added.

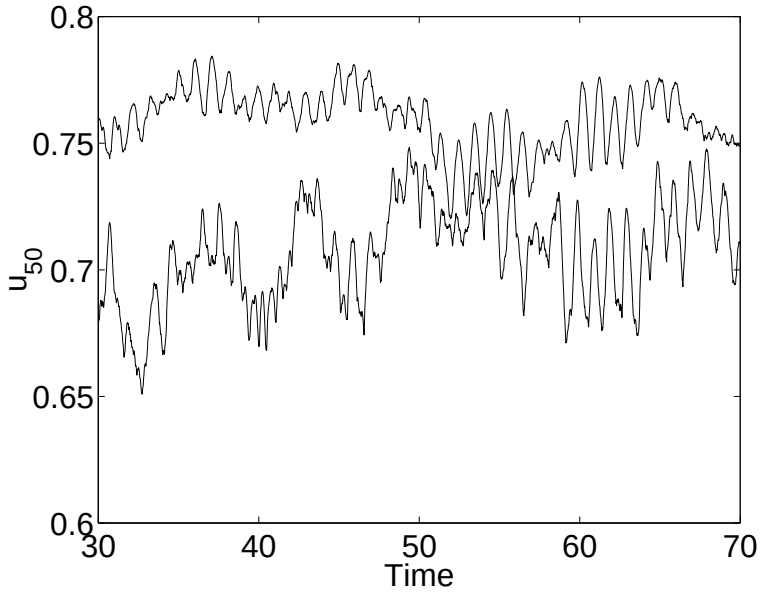


Figure 8: $u_i(t)$ at the center of a bump for $\beta = 0.9$ (upper line) and $\beta = 1.9$ (lower line) for $I = 0.9$, $J_{ij}$ as in Fig. 1, and noise as in Fig. 3. As $\beta$ increases, the size of the noisy oscillations increases.

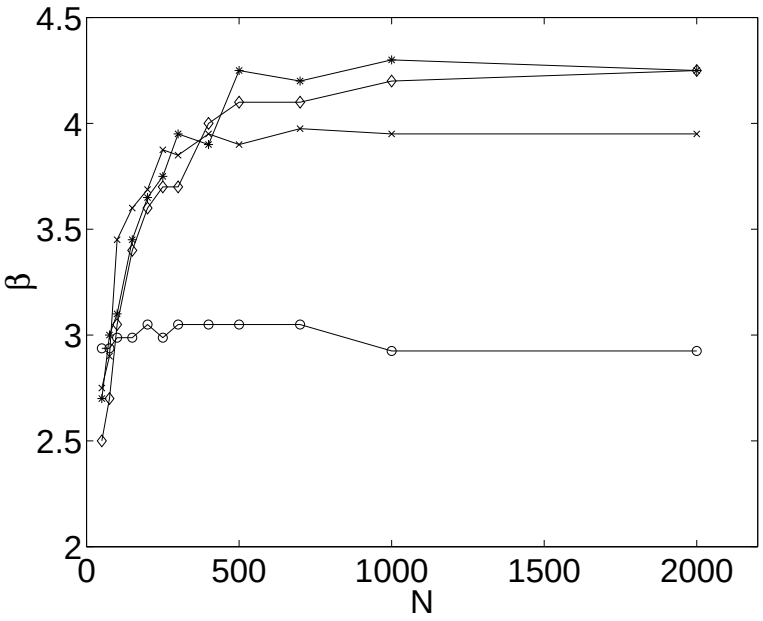


Figure 9: Values of $\beta$ above which the bump is not stable as a function of $N$ in the network for $I = 0.91$, $J_{ij}$ as in Fig. 1, and the mean frequencies of the random current pulses have values: no noise ($\circ$), 0.05 ($\times$), 0.1 ($*$), and 0.2 ($\diamond$).

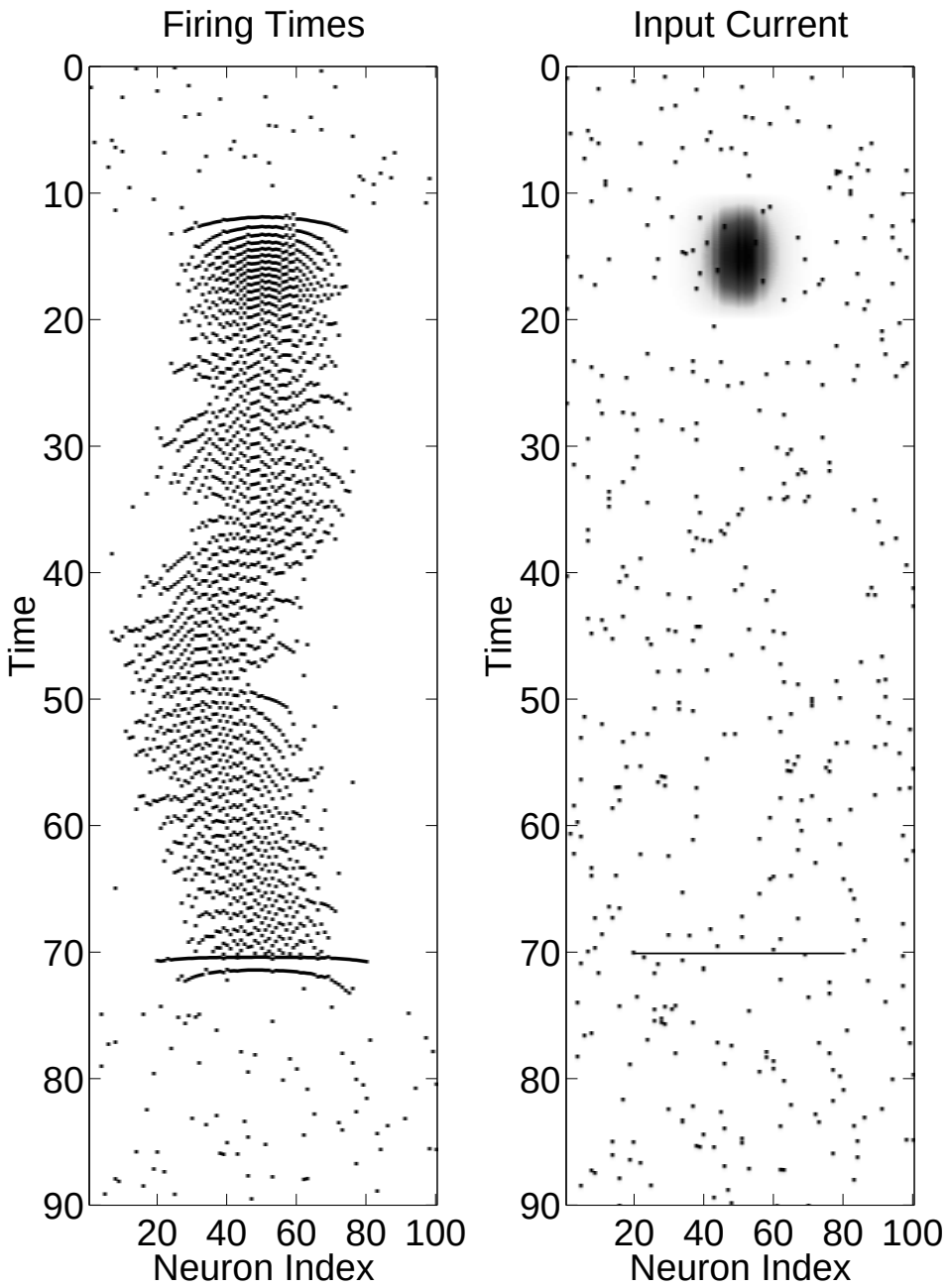


Figure 10: Turning on and off a bump with excitation. The plot on the left shows the firing times and that on the right shows the input current (maximum amplitude above background 0.4). The coupling weight is as in Fig. 1, $\beta = 2.4$, $I = 0.9$ and noise is as in Fig. 3.